Requirement of Rsk-2 for Epidermal Growth Factor-Activated Phosphorylation of Histone H3

the *MID1* mRNA by Northern blotting as in (*26*). The transfected cells were seeded in 100-mm dishes for immunoblotting, or in 35-mm dishes containing cover slips or in 4-cm² silicon chambers coated with fibronectin (50 µg/ml) for $[Ca^{2+}]_c$ measurements. To transiently induce expression of the *MID1* gene, 80 µM $ZnCl_2$ was added to the medium.

6. M. Kanzaki et al., unpublished data.

7. The $[Ca^{2+}]_c$ of cells grown on cover slips was monitored by use of fura-2 as in (*25*). Briefly, cells cultured on a cover slip were incubated with 2 µM fura-2/acetoxymethyl ester (AM) (Dojin, Kumamoto, Japan) for 20 min at room temperature, and then each cover slip was examined by fluorescence microscopy, with the fluorescence measured using the ARGUS calcium imaging system (Hamamatsu Photonics, Hamamatsu, Japan).

8. M. Kanzaki *et al.*, unpublished data.

9. M. Kanzaki *et al.*, unpublished data.

10. We used the single-channel variation on the cell-attached patch-clamp technique for analysis of Mid1 molecule unitary channel events and measured changes in membrane currents with the whole-cell mode of the patch-clamp technique, as in (*26*). The resistance of the patch pipettes was 4 to 6 megohms for whole-cell analysis and 7 to 7.5 megohms for single-channel analysis, and the indifferent electrode was an Ag-AgCl plug connected to the bath via a KCl agar bridge. All experiments were done at 22° to 26°C. For whole-cell patch-clamp analysis, the pipette solution contained 120 mM *N*-methyl-D-glutamate (NMDG)–aspartate, 10 mM HEPES (pH 7.0), and 1 mM EGTA. The bath solution contained 120 mM NMDG-aspartate, 10 mM Ca(OH)₂, and 10 mM HEPES (pH 7.4 adjusted with aspartate). The osmolarity of these solutions was adjusted to 320 mosM with sucrose. Cells were held at 0 mV, and the *I-V* relations were recorded using jump pulses of 20 mV from -100 mV to $+100$ mV for 400 ms at an interval of 1 s.

11. M. Kanzaki *et al.*, unpublished data.

12. To evaluate permeability of monovalent cations, the pipette solution contained 150 mM Cs^+-gluconate, 1 mM EGTA, 10 mM HEPES (pH 7.2). The bath solution contained 150 mM Cs^+-, K^+- or Na^+-gluconate and 10 mM HEPES (pH 7.4). The *I-V* relations were obtained by applying voltage pulses as mentioned above. The osmolarity of these solutions was adjusted to 320 mosM with sucrose.

13. M. Kanzaki *et al.*, unpublished data.

14. For the single-channel analysis, seals of ~20 gigohm were achieved by applying slightly negative pressure (~5 cm H_2O) in the patch pipette, and after formation of a stable seal, the suction in the pipette was released, establishing a reference point for zero applied pressure. To investigate mechanosensitivity of Mid1, negative hydrostatic pressures of up to 40 cm H_2O were applied. The total number of functional channels (N) in the patch was estimated by observing the number of peaks detected on the amplitude histogram. As an index of channel activity, NPo (the number of channels times the open probability) was calculated as in [M. Kanzaki, M. A. Lindorfer, J. C. Garrison, I. Kojima, *J. Biol. Chem.* **272**, 14733 (1997)]. Kinetics of open and closed events were analyzed for patches containing only one active channel (determined by an all-points amplitude histogram).

15. M. Kanzaki *et al.*, unpublished data.

16. M. C. Gustin, X.-L. Zhou, B. Martinac, C. A. Kung, *Science* **242**, 762 (1988).

17. M. B. Jackson, *Methods Enzymol.* **207**, 729 (1992).

18. Single-channel currents were measured in inside-out patches with 150 mM CsCl, 1 mM EGTA-Cs, and 10 mM HEPES-Cs (pH 7.4) for the pipette solution and 150 mM KCl, 3 mM EDTA-K, and 10 mM HEPES-K (pH 7.4) for the bath solution. Membrane potential was held at–60 mV and negative pressure (0 to 40 cm H_2O) was applied.

19. K. Naruse, T. Yamada, M. Sokabe, *Am. J. Physiol.* **274**, H1532 (1998); K. Naruse and M. Sokabe, *ibid.* **264**, C1037 (1993).

20. Mid1-expressing CHO cells were removed from the dish containing 0.01% EDTA and 0.02% trypsin and transferred to a 4-cm² silicon chamber coated with fibronectin (50 µg/ml), at a density of 4 × 10⁴ to 5 × 10⁴ cells/cm². The silicon chamber had a 100-µm-thick transparent bottom with 5-mm-thick side walls to prevent narrowing its bottom center. The silicon chamber was attached to a stretching apparatus that was driven by a computer-controlled stepping motor. Using this system, we could apply quantitative and uniform stretch to most of the cells on the bottom, and lateral thinning did not exceed 1% at 120% stretch (*19*). After cells were allowed to attach to the chamber bottom overnight, $ZnCl_2$ was added (80 µM, final concentration) to induce the expression of Mid1. After 12 hours of incubation, Mid1-expressing CHO cells on a silicon membrane were incubated with 1 µM fura-2/AM (Molecular Probes, Eugene, OR) for 15 min and for another 15 min in a solution containing 140 mM NaCl, 5 mM KCl, 2 mM $CaCl_2$, 10 mM glucose, and 10 mM HEPES (pH 7.40) as in (*19*). A single uniaxial-stretch pulse (2 s duration, 120% peak to peak) was applied. The $[Ca^{2+}]_c$ was measured by using a fluorescence microscope (M1000; Inter Dec Ltd., Osaka, Japan) with a 20× objective (Nikon, Fluor 20). The area of interest was 5 × 10⁴ µm², and the number of cells was ~60.

21. M. Kanzaki *et al.*, unpublished data.

22. H. Iida, Y. Yagawa, Y. Anraku, *J. Biol. Chem.* **265**, 13391 (1990); L. Marsh and M. D. Rose, in *The Molecular and Cellular Biology of the Yeast* Saccharomyces, J. R. Pringle, J. R. Broach, E. W. Jones, Eds. (Cold Spring Harbor Laboratory Press, New York, 1997), pp. 827–888.

23. Y. Tasaka *et al.*, unpublished data.

24. S. Moreno, A. Klar, P. Nurse, *Methods Enzymol.* **194**, 795 (1991).

25. M. Kanzaki, H. Shibata, H. Mogami, I. Kojima, *J. Biol. Chem.* **270**, 13099 (1995).

26. M. Kanzaki, L. Nie, H. Shibata, I. Kojima, *ibid.* **272**, 4964 (1997).

27. Single-letter abbreviations for the amino acid residues are as follows: A, Ala; C, Cys; D, Asp; E, Glu; F, Phe; G, Gly; H, His; I, Ile; K, Lys; L, Leu; M, Met; N, Asn; P, Pro; Q, Gln; R, Arg; S, Ser; T, Thr; V, Val; W, Trp; and Y, Tyr.

28. Supplementary materials are available at www.sciencemag.org/feature/data/1038393.shl

29. We thank S. Ozawa (Gunma University) for helpful discussion. Supported in part by Grants-in-Aid for Scientific Research on Priority Areas to H.I. and I.K., Grant-in-Aid for Scientific Research (C) to H.I., and Grant-in-Aid for Scientific Research (B) to M.S. from the Ministry of Education, Science, Sports and Culture of Japan, and by a grant from the Yamada Science Foundation to H.I., from ETL to C.S., from Japan Space Forum to I.K. and M.S., and from CREST to M.S.

12 January 1999; accepted 28 June 1999

Requirement of Rsk-2 for Epidermal Growth Factor–Activated Phosphorylation of Histone H3

Paolo Sassone-Corsi,[1]*† Craig A. Mizzen,[2]† Peter Cheung,[2] Claudia Crosio,[1] Lucia Monaco,[1] Sylvie Jacquot,[1] André Hanauer,[1] C. David Allis[2]*

During the immediate-early response of mammalian cells to mitogens, histone H3 is rapidly and transiently phosphorylated by one or more unidentified kinases. Rsk-2, a member of the pp90[rsk] family of kinases implicated in growth control, was required for epidermal growth factor (EGF)–stimulated phosphorylation of H3. *RSK-2* mutations in humans are linked to Coffin-Lowry syndrome (CLS). Fibroblasts derived from a CLS patient failed to exhibit EGF-stimulated phosphorylation of H3, although H3 was phosphorylated during mitosis. Introduction of the wild-type *RSK-2* gene restored EGF-stimulated phosphorylation of H3 in CLS cells. In addition, disruption of the *RSK-2* gene by homologous recombination in murine embryonic stem cells abolished EGF-stimulated phosphorylation of H3. H3 appears to be a direct or indirect target of Rsk-2, suggesting that chromatin remodeling might contribute to mitogen-activated protein kinase–regulated gene expression.

In mammalian cells, various environmental stimuli induce a Ras-dependent MAP (mitogen-activated protein) kinase cascade that results in the transcriptional activation of immediate-early–responsive genes (*1*, *2*). These transcriptional responses are thought to depend on modulation of the nuclear localization, DNA binding, and activation properties of transcription factors, but the roles of MAPK phosphorylation in this process remain poorly defined (*1*).

Remodeling of chromatin structure appears to have a primary role in transcriptional regulation (*3*), and posttranslational modifications of histones are thought to contribute to this remodeling. Widespread phosphorylation of histones, particularly histones H1 and H3, correlates with mitosis in many cells

¹Institut de Génétique et de Biologie Moléculaire et Cellulaire, CNRS, INSERM, ULP, B. P. 163, 67404 Illkirch-Strasbourg, France. ²Department of Biochemistry and Molecular Genetics, University of Virginia, Charlottesville, VA 22908, USA.

*To whom correspondence should be addressed. E-mail: paolosc@igbmc.u-strasbg.fr; allis@virginia.edu
†These authors contributed equally to this work. The contributions of the Sassone-Corsi and Allis labs were equal.

(*4*). Additionally, rapid and transient phosphorylation of a subset of histone H3 molecules correlates with the activated expression of immediate-early genes such as c-*fos* and c-*jun* in mammalian cells after mitogen stimulation (*5*). These observations suggest that H3 phosphorylation may contribute to chromatin remodeling during mitosis and transcriptional activation.

We have described a polyclonal antiserum (pS10) to a synthetic peptide mimic of histone H3 monophosphorylated at serine-10 that recognizes H3 phosphorylated during mitosis (*6*). To determine whether the pS10 antiserum detects mitogen-stimulated phosphorylation of H3, we isolated histones from mouse fibroblasts deprived of serum and then treated with a buffer control or EGF. The proteins were resolved by SDS–polyacrylamide gel electrophoresis (PAGE), transferred to a polyvinylidene difluoride (PVDF) membrane, and probed with pS10 antiserum. A rapid and transient increase in phosphorylation of H3 was detected in EGF-treated cells but not in unstimulated cells (Fig. 1A). Similar results were obtained when tetradecanoyl phorbol acetate was used in place of EGF (*7*, *8*).

To identify kinases that mediate EGF-dependent phosphorylation of histone H3, we used kinase activity gel assays with purified histone H3 or H3 NH₂-terminal peptide substrates to detect H3-specific kinases. We consistently detected H3 phosphorylation by a polypeptide with an apparent molecular size of ~90 kD in nuclear extracts from EGF-stimulated cells that was not detected in extracts from quiescent cells (Fig. 1B). This activity did not appear to be due to kinase autophosphorylation because phosphorylation was not detected when identical samples were analyzed on gels containing bovine serum albumin instead of H3 (*9*).

The molecular size and activation by EGF stimulation suggested that the catalytically active species might be a member of the pp90^{rsk} (ribosomal S6 kinase) family of mitogen-activated serine-threonine kinases implicated in cell proliferation and differentiation (*10*). To test this hypothesis, nuclear extracts were run on an H3 kinase activity gel, and a portion of each gel lane encompassing the 90-kD region was excised immediately after electrophoresis. Proteins in these gel strips were subjected to electrophoresis on a second SDS gel and analyzed by immunoblotting with antiserum to pp90^{rsk}. Consistent with the known nuclear localization of pp90^{rsk} isoforms after mitogenic stimulation (*11*), an immunoreactive band with electrophoretic mobility similar to that of the kinase apparent in the activity gel was detected in nuclear extracts from EGF-stimulated, but not unstimulated, cells (Fig. 1C).

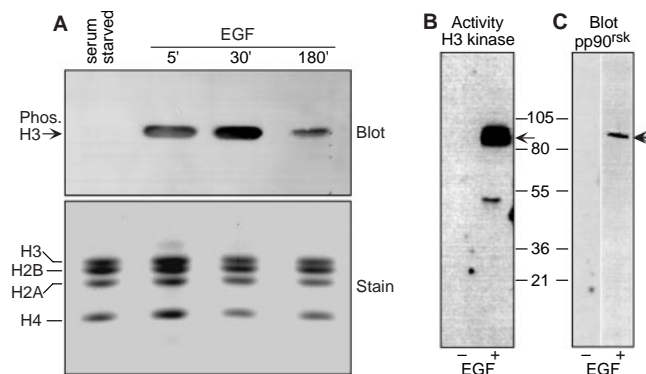The pp90^{rsk} proteins phosphorylate several different protein substrates in vitro (*10*). In mammals, the pp90^{rsk} family comprises three functionally nonredundant isoforms: Rsk-1, Rsk-2, and Rsk-3 (*12*) [also referred to as MAPKAP-K1a, b, and c, respectively (*2*)]. We found that biochemically purified rabbit Rsk-2 [containing little or no Rsk-1 and Rsk-3 (*13*)] phosphorylated only histone H3 in both free histone and nucleosomal substrates (Fig. 2A). H3 phosphorylated by Rsk-2 in vitro was recognized by the pS10 antiserum (Fig. 2A), and microsequence analysis confirmed that Ser-10 is the only site in the NH₂-terminus of H3 phosphorylated by Rsk-2 in vitro (Fig. 2B).

Because mutations in Rsk-2, but not Rsk-1 or Rsk-3, are associated with CLS (*14*), we compared pS10 staining of Epstein-Barr virus (EBV)–transformed fibroblasts derived from a CLS patient with that of similarly transformed control fibroblasts from an unaffected sibling. After stimulation with EGF, phosphorylated H3 was distributed in nuclei of normal (control) cells in a speckled pattern (Fig. 3) similar to that reported for mitogen-stimulated mouse fibroblasts (*8*). In contrast, nuclear staining was not detected in interphase CLS cells even though mitotic chromosomes were stained in CLS cells undergoing mitosis (Fig. 3). These data indicate that H3 is a target of (at least) two distinct signaling pathways: one that is dependent on Rsk-2 and linked to activation by EGF, and another that is Rsk-2-independent and associated with mitosis.

Immunoblot analyses confirmed that H3 phosphorylation was not readily detected in serum-starved or EGF-treated CLS fibroblasts (Fig. 4A), nor was it detected after stimulation of these cells with serum or ultraviolet (UV) irradiation (*9*). A weak signal, equivalent in serum-starved and EGF-stimulated CLS cells, which we attribute to mitotic

Fig. 1. Correlation of EGF-activated histone H3 phosphorylation with increased activity of a 90-kD H3 kinase in nuclear extracts. (**A**) NIH 3T3 mouse fibroblasts were serum-starved and then stimulated with EGF for 5, 30, or 180 min (*24*). (Upper) pS10 immunoblot of acid-soluble nuclear proteins resolved by SDS-PAGE (*25*). The corresponding region of a gel run in parallel and stained with Coomassie blue is shown in the lower panel. (**B**) Equivalent amounts of nuclear extract from NIH 3T3 cells after serum-starvation (−EGF) and after EGF treatment for 30 min (+EGF) were resolved by SDS-PAGE in an 8% gel containing histone H3 and processed to detect kinase activity (*25*, *26*). The arrow denotes a band in the autoradiogram with an apparent molecular mass similar to that of pp90^{rsk}, as shown in (C). The identity of the band at 50 kD is not known. (**C**) Parallel in-gel H3 kinase assays were performed as in (B) except that after electrophoresis, the 90-kD region for each sample was excised and again subjected to electrophoresis on a second SDS gel. The arrow denotes the position of pp90^{rsk} detected when this second gel was analyzed by immunoblotting with pp90^{rsk} antiserum.

Fig. 2. Preferential phosphorylation of histone H3 by Rsk-2 in vitro. (**A**) Free histones (Free) or mononucleosomes (Nuc.) were incubated with rabbit Rsk-2 in vitro (*27*). These reactions were then resolved by SDS-PAGE (12% gel) and analyzed by Coomassie blue staining, autoradiography and protein immunoblotting with pS10 antiserum. (**B**) After incubation with [γ-³²P]ATP and rabbit Rsk-2, histone H3 was recovered by rpHPLC and subjected to NH₂-terminal microsequencing analysis (*28*). About 50% of the products from each sequencing cycle were collected for liquid scintillation counting and the remainder used for residue identification by HPLC. The *y*-axis values represent total ³²P cpm eluted in each sequencing cycle plotted as a function of the residue identified in that cycle.
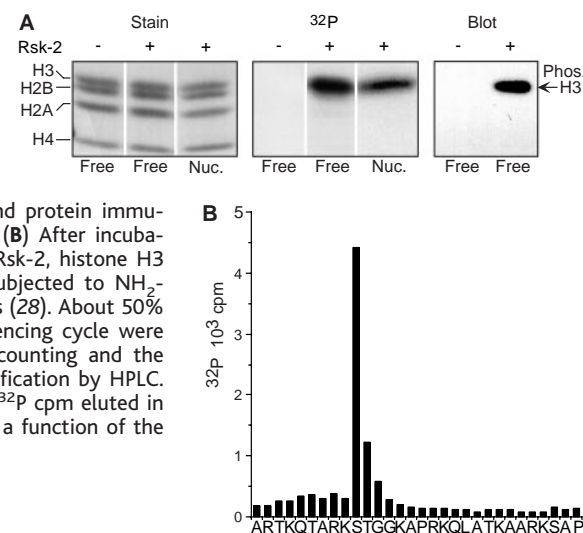
H3 phosphorylation in these slowly growing cultures, was detected only after lengthy exposures (*9*). Because the amounts of Rsk-1 and Rsk-3 expressed in these fibroblasts and several CLS lymphoblast lines are equivalent to those in normal cells (*14*, *15*), these results suggest that the Rsk-1 and Rsk-3 isoforms are unable to compensate for the loss of Rsk-2 function.

Phosphorylation of histone H3 was observed in both serum-starved and EGF-stimulated cultures of the EBV-transformed control fibroblasts (Fig. 4A). This might reflect increased proliferation of these cells upon transformation. To test this hypothesis, we treated cultures with aphidicolin and nocodazole to arrest these cells in mitosis and monitored EGF-stimulated phosphorylation of H3 after releasing cultures from this cell cycle block. Augmented phosphorylation of H3 was observed in nocodazole-arrested cells (Fig. 4B). Six hours after releasing cells into serum-free medium, phosphorylation of H3 was not observed, regardless of whether cells were stimulated with EGF or not. However, by 24 hours, EGF treatment induced phosphorylation of H3 (Fig. 4B). Stimulation with serum or UV irradiation induced similar amounts of H3 phosphorylation in parallel cultures at this point (*9*). The low amount of phosphorylated H3 detected in unstimulated cells at 24 hours (Fig. 4B) may represent mitotic phosphorylation of H3 as the synchrony of cultures declined over time. Mitogenic induction of c-*fos* expression and MAPK signaling are conserved in these cells (*15*); thus, the H3 phosphorylation observed in asynchronous cultures of these cells may mask the mitogenic H3 phosphorylation response but appears not to be associated with alterations in mitogen response pathways per se.

Rsk-2 immunoprecipitates from serum-supplemented control cells contained more H3 kinase activity than immunoprecipitates prepared in parallel from CLS cells (*9*). When immunoprecipitates from control cells were analyzed, bands migrating just ahead of a rabbit Rsk-2 standard were detected on an H3 kinase activity gel and on a parallel Rsk-2 immunoblot (Fig. 4C). The heterogeneity resolved on the activity gel may reflect MAPK phosphorylation of Rsk-2. In contrast, Rsk-2 was not detected in the immunoprecipitate from CLS cells by immunoblotting, and a weak H3 kinase activity was barely detected in activity gels (Fig. 4C). Although the absence of Rsk-2 in immunoblots is consistent with the expectation that Rsk-2 protein expressed in these cells lacks the COOH-terminal epitopes recognized by the antiserum to Rsk-2 (*14*, *15*), attempts to detect Rsk-2 expression in these cells with antiserum to an NH$_2$-terminal epitope of pp90^{rsk} were also unsuccessful (*15*). Thus, the weak signal in the activity gel associated with the Rsk-2 immunoprecipitate from CLS cells may be attributable to contaminating kinases, possibly Rsk-1 or Rsk-3. Other bands were not apparent in any of the samples, and the activity observed was not due to kinase autophosphorylation because activity was not detected when immunoprecipitates were assayed in activity gels prepared without protein substrate (*7*). We conclude that the H3 kinase activity in immunoprecipitates from normal cells was intrinsic to Rsk-2, and that H3

Fig. 3. Effects of Rsk-2 deficiency on mitogen-stimulated but not mitotic phosphorylation of histone H3 in CLS cells. Representative fields from indirect immunofluorescence microscopy of transformed normal (upper) and CLS (middle) human fibroblasts, stimulated for 30 min with EGF and costained with DAPI and pS10 antiserum (*23*, *24*), are shown in the left and right panels, respectively. The punctate nuclear localization of phosphorylated H3 in the normal cells (open arrowheads) is indicated. The lower pair of panels shows a second field of CLS fibroblasts in which a cell in mitosis (arrowheads) is visible.
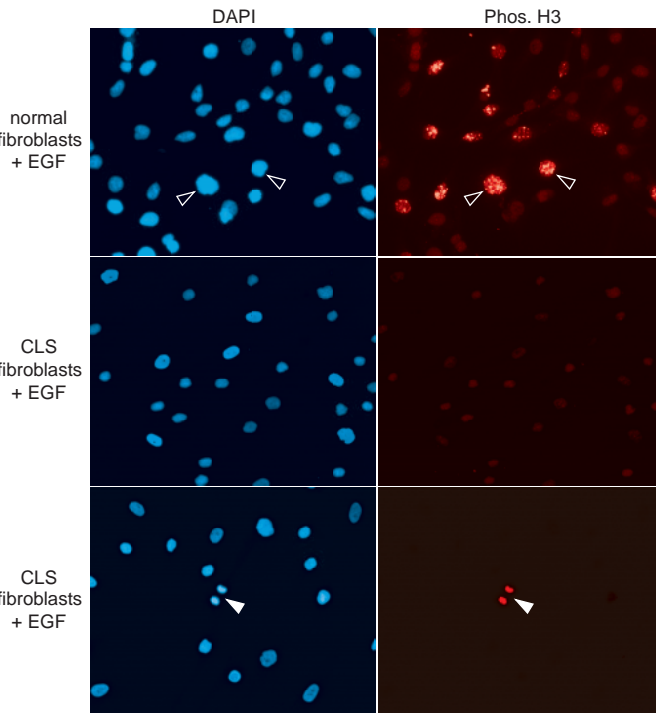

Fig. 4. Deficiency in EGF-stimulated phosphorylation of histone H3 and Rsk-2–associated H3 kinase activity in CLS cells. (**A**) Transformed normal and CLS human fibroblasts were dissolved in sample buffer containing SDS, resolved by SDS-PAGE (12% gel), and analyzed by immunoblotting with the pS10 antiserum and anti-tubulin (*22*). Phosphorylated H3 was detected in normal cells after serum starvation (−) and after the addition of EGF. The high level of phosphorylated H3 detected in these cells after serum deprivation appears to be associated with transformation-induced proliferation [see (B) and text]. Phosphorylated H3 was not detected in Rsk-2–deficient CLS cells regardless of the presence or absence of EGF. Tubulin levels demonstrate equivalent loading. (**B**) Transformed normal human fibroblasts [as in (A)] were synchronized by using coupled aphidicolin and nocodazole treatments (*29*). Metaphase-arrested cells were released into serum-free media and harvested 6 or 24 hours later with or without exposure to EGF for 30 min. Cells were dissolved in sample buffer containing SDS, resolved by SDS-PAGE (10% gel), and analyzed by immunoblotting with the pS10 antiserum and anti-CREB. The strong induction of H3 phosphorylation by EGF treatment 24 hours after release of the cells from mitotic arrest is apparent. CREB levels demonstrate equivalent loading. (**C**) Anti–Rsk-2 immunoprecipitates were prepared from whole-cell extracts of randomly growing transformed normal human and CLS fibroblasts as described (*14*). Immunoprecipitates were solubilized by boiling in SDS-PAGE sample buffer, and a portion (90%) of the material released was analyzed on a kinase activity gel containing purified H3 (left) (*26*). The remaining 10% of the released material was resolved on an SDS-PAGE gel and analyzed by protein immunoblotting with Rsk-2–specific antiserum (right). Rabbit skeletal muscle Rsk-2 (0.05 U) was used as a positive control (std). H3 kinase activity is markedly diminished in the CLS Rsk-2 immunoprecipitate.
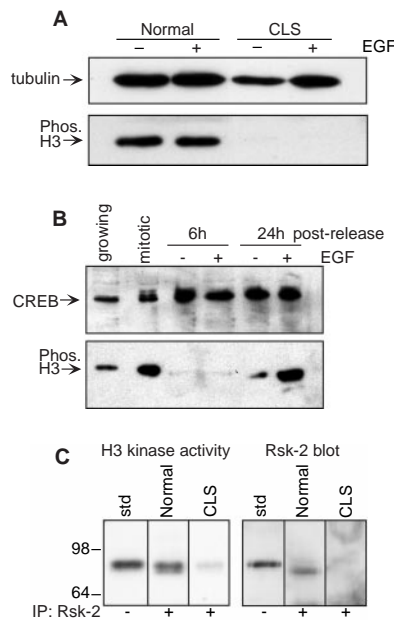
kinase activity in immunoprecipitates from CLS cells was diminished due to the lesion in the *RSK-2* locus in this patient.

We assayed whether ectopic expression of Rsk-2 could restore mitogen-stimulated phosphorylation of histone H3 in CLS cells. Phosphorylation of H3 in response to EGF was detected in CLS fibroblasts transfected with *RSK-2* DNA but not in cells transfected with vector DNA alone, even though MAPK was activated by phosphorylation upon EGF stimulation in both cell cultures (Fig. 5A). Changes in the amounts of Rsk-1 and Rsk-3 were not observed upon Rsk-2 expression (Fig. 5A). Furthermore, CLS fibroblasts transfected with *RSK-2* DNA, but not those transfected with vector DNA alone, displayed punctate nuclear pS10 staining after EGF treatment (Fig. 5B). These results argue strongly that Rsk-2 can directly or indirectly mediate EGF-stimulated phosphorylation of H3 in vivo.

RSK-2 mutations are closely associated, if not causally linked, to CLS (*16*). However, because mutations at additional loci may contribute to defects in mitogen-responsiveness in CLS cells, we specifically disrupted the *RSK-2* gene in murine embryonic stem (ES) cells by homologous recombination (*17*) and assayed these cells for EGF-stimulated phosphorylation of histone H3. The absence of Rsk-2 expression in these cells was confirmed by protein immunoblotting (Fig. 6A), and disruption of the endogenous *RSK-2* gene was confirmed by Southern (DNA) blot analyses (*17*). Augmented phosphorylation of H3 was detected by immunoblotting after EGF stimulation of serum-deprived wild-type (wt) ES cells (Fig. 6B). In contrast, no stimulation of H3 phosphorylation in response to EGF was detected in Rsk-2⁻ ES cells even though

MAPK was activated in these cells after EGF treatment (Fig. 6B). The amount of phosphorylated H3 in serum-deprived and EGF-stimulated Rsk-2⁻ ES cells was similar to that in serum-deprived wt ES cells. Thus, EGF-stimulated phosphorylation of H3 requires Rsk-2.

Fig. 6. Rsk-2 is required for EGF-stimulated phosphorylation of histone H3 in mouse cells. (**A**) Confluent wild-type (wt ES) and Rsk-2–deficient (Rsk-2⁻) cells (*17*) were starved for 48 hours in 0.5% FBS and then stimulated with EGF (30 ng/ml) for 30 min. Cells were dissolved in boiling SDS buffer and resolved on a 10% SDS-PAGE gel. Expression of Rsk-1, Rsk-2, and Rsk-3 was then analyzed by immunoblotting with isoform-specific antisera (*13*). (**B**) Samples prepared as in (A) from serum-deprived (−EGF) and EGF-stimulated (+EGF) wild-type and Rsk-2⁻ ES cells were resolved on a 10% SDS-PAGE gel, and the levels of MAPK (ERK1/ERK2), phosphorylated MAPK, H3, and phosphorylated H3 were assessed by immunoblotting with the respective antisera (*13*). EGF stimulated MAPK phosphorylation in both wt and Rsk-2⁻ cells, but H3 phosphorylation was deficient in Rsk-2⁻ cells. The levels of (nonphosphorylated) H3 and MAPK confirm equivalent loading. (**C**) Randomly growing wild-type (upper) and Rsk-2⁻ (lower) ES cells were costained with DAPI and pS10 antiserum (left and right panels, respectively). Solid arrowheads indicate cells in mitosis. Phosphorylated H3 was localized in mitotic chromosomes of both wild-type and Rsk-2⁻ cells, but punctate nuclear localization was apparent only in interphase wild-type ES cells (open arrowheads).
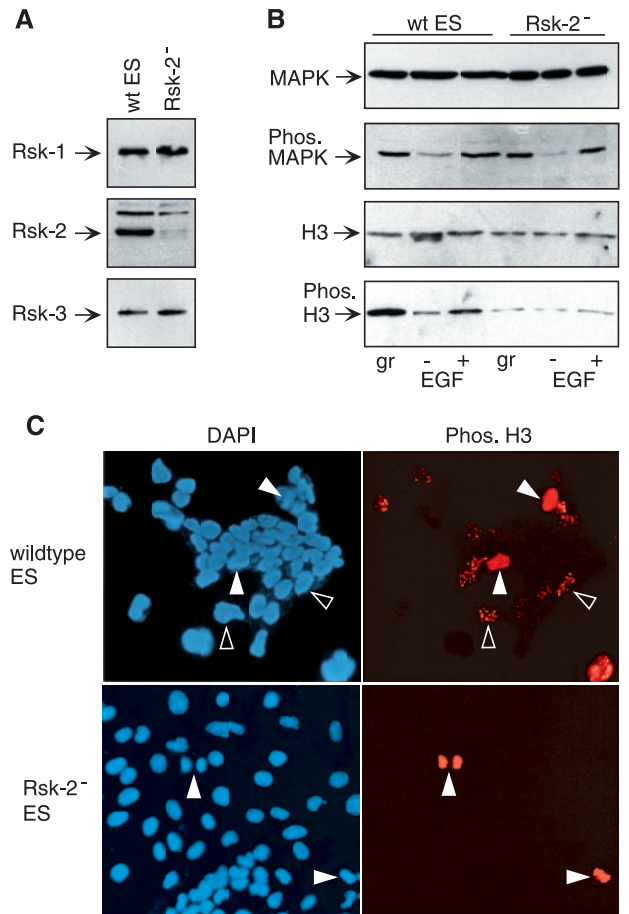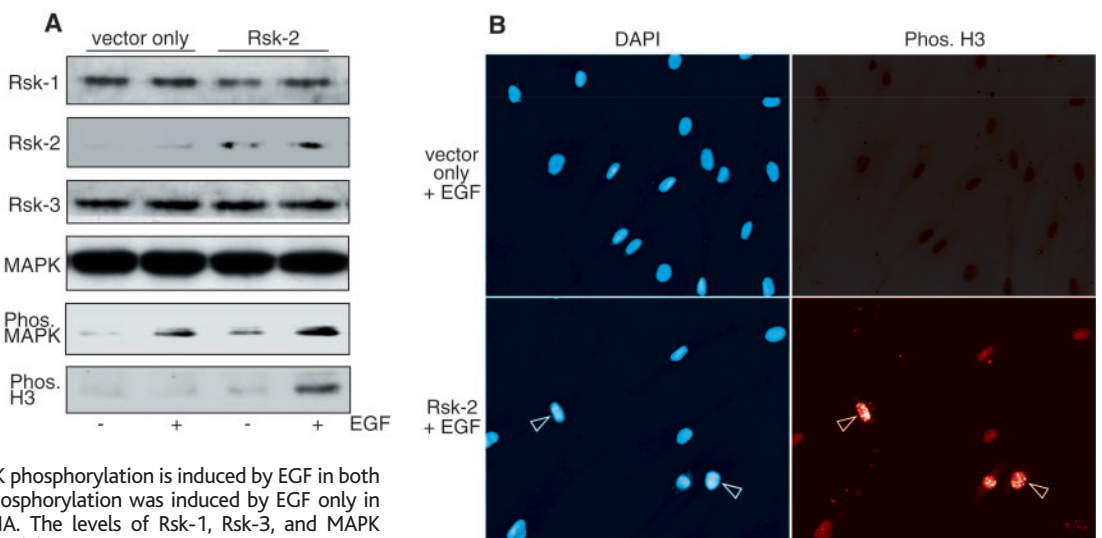

Fig. 5. Restoration of mitogen-stimulated phosphorylation of histone H3 in CLS cells after ectopic expression of Rsk-2. (**A**) After transfection with a human Rsk-2 expression vector (Rsk-2) or the empty vector (vector only), CLS fibroblasts were serum-starved and mock-treated (−EGF) or treated with EGF for 30 min (+EGF) and dissolved in boiling SDS buffer (*30*). Cellular proteins were resolved on 12% SDS-PAGE gels, and the expression of the indicated proteins was analyzed by immunoblotting with the respective antisera (*13*). Although MAPK phosphorylation is induced by EGF in both types of transfected cells, H3 phosphorylation was induced by EGF only in cells transfected with Rsk-2 DNA. The levels of Rsk-1, Rsk-3, and MAPK demonstrate equivalent loading. (**B**) Representative fields from indirect immunofluorescence microscopy of CLS fibroblasts that were serum-starved and stimulated with EGF for 30 min after transfection with a human Rsk-2 expression vector (lower) or the empty vector (upper) as in (A). Cells costained with DAPI and pS10 antiserum are shown on the left and right, respectively. The punctate nuclear localization of phosphorylated H3 in the Rsk-2-transfected cells (open arrowheads) is indicated.

These observations were confirmed by pS10 staining in randomly growing wt and Rsk-2⁻ ES cells. Punctate nuclear staining resembling that described above for normal human fibroblasts was observed in cultures of wt ES cells, but not in cultures of Rsk-2⁻ ES cells (Fig. 6C). Mitotic phosphorylation of H3 in murine cells appears to be independent of Rsk-2 because it was readily detected in both wt and Rsk-2⁻ ES cells (Fig. 6C), in agreement with our data for human fibroblasts (Fig. 3).

Our results indicate that Rsk-2 is required for EGF-stimulated phosphorylation of histone H3 in vivo. However, the role of H3 phosphorylation in cellular responses to mitogens remains to be defined. Although activation of cAMP response element–binding protein (CREB) phosphorylation and c-*fos* transcription (whose promoter contains a CREB recognition site) by EGF are defective in CLS cells (*15*), these same cells resemble normal cells in other responses to mitogenic and other stimuli (*15*). Thus, it appears that Rsk-2 ablation does not lead to global changes in the activity of other signaling pathways. Furthermore, our finding that EGF-activated phosphorylation of H3 is Rsk-2–dependent whereas EGF-induced phosphorylation of Elk-1 and serum response factor in CLS cells is not (*15*), indicates that not all MAPK-regulated nuclear responses require Rsk-2.

Evidence for the direct involvement of H3 phosphorylation in gene activation is limited (*8*). However, a growing body of evidence indicates that conserved regulatory pathways have evolved in eukaryotes wherein chromatin-modifying activities, notably histone acetylases and deacetylases, are recruited to specific promoters through selective interactions with activator and coactivator proteins (*18*). The growth factor–dependent interaction of pp90^rsk with the transcriptional coactivator CBP (*19*), a histone acetyltransferase (*20*), raises the possibility that histone acetylation and phosphorylation may act together to facilitate gene expression at mitogen-responsive promoters such as c-*fos* and c-*jun* (*5*, *21*).

References and Notes

1. R. Treisman, *Curr. Opin. Cell Biol.* **8**, 205 (1996).
2. P. Cohen, *Trends Cell Biol.* **7**, 353 (1997).
3. G. Felsenfeld, *Cell* **86**, 13 (1996); A. P. Wolffe, *Biochem. Soc. Trans.* **25**, 354 (1997).
4. E. M. Bradbury, *Bioessays* **14**, 9 (1992); D. Koshland and A. Strunnikov, *Annu. Rev. Cell Dev. Biol.* **12**, 305 (1996).
5. L. C. Mahadevan, A. C. Willis, M. J. Barratt, *Cell* **65**, 775 (1991); M. J. Barratt, C. A. Hazzalin, E. Cano, L. C. Mahadevan, *Proc. Natl. Acad. Sci. U.S.A.* **91**, 4781 (1994).
6. M. J. Hendzel et al., *Chromosoma* **106**, 348 (1997).
7. C. D. Allis et al., unpublished data.
8. D. N. Chadee et al., *J. Biol. Chem.*, in press.
9. P. Sassone-Corsi et al., unpublished data.
10. J. Blenis, *Proc. Natl. Acad. Sci. U.S.A.* **90**, 5889 (1993).
11. Y. Zhao, C. Bjorbaek, S. Weremowicz, C. C. Morton, D. E. Moller, *Mol. Cell. Biol.* **15**, 4353 (1995); R. H. Chen, C. Sarnecki, J. Blenis, ibid. **12**, 915 (1992).
12. Y. Zhao, C. Bjorbaek, D. E. Moller, *J. Biol. Chem.* **271**, 29773 (1996).
13. Antisera to Ser-10–phosphorylated H3 (pS10) (*6*), CREB, phospho-CREB, and MAPK (ERK1/ERK2) were from Upstate Biotechnology. Antisera to Rsk-1, Rsk-2, and Rsk-3 and peroxidase-conjugated donkey anti-goat secondary antibody were from Santa Cruz. Anti-pp90^rsk was from Transduction Labs. Anti–phospho-MAPK was from New England BioLabs. Anti-tubulin was from Sigma. Peroxidase-conjugated donkey anti-rabbit and peroxidase-conjugated sheep anti-mouse secondary antibodies and ECL+ reagents were from Amersham. Biochemically purified rabbit Rsk-2 was from Upstate Biotechnology. Only minor contamination by Rsk-1 and Rsk-3 was detected in the preparation (lot 13479) used here by immunoblotting with Rsk isoform-specific antisera.
14. E. Trivier et al., *Nature* **384**, 567 (1996).
15. D. De Cesare, S. Jacquot, A. Hanauer, P. Sassone-Corsi, *Proc. Natl. Acad. Sci. U.S.A.* **95**, 12202 (1998).
16. S. Jacquot et al., *Am. J. Hum. Genet.* **63**, 1631 (1998).
17. S. Jacquot, P. Sassone-Corsi, A. Hanauer, unpublished data. The Rsk-2 gene was interrupted by a neomycin cassette (lox-pGK-neo-lox) followed by stop codons in exon 2. The construct was electroporated into ES cells and transformants selected by using G418. Genomic DNA from G418-resistant ES clones was extracted and tested for homologous recombination by Southern analysis [A. Dierich and P. Dolle, in *Methods in Developmental, Toxicology and Biology* (Blackwell Science, Oxford, 1997), pp. 111–123]. As the murine ES cells used for gene targeting are male cells, and as the Rsk-2 gene is on the X-chromosome (*14*), the homologous recombination event generates cells deficient in Rsk-2 protein. Wild-type (ES clones resistant to G418 due to integration of the neomycin cassette at loci other than *RSK-2*) and Rsk-2-deficient ES cells were grown on a feeder layer of fibroblasts in the presence of leukemia inhibitory factor. Feeder cells were eliminated by exposure to G418 over 4 days before all treatments to ensure that only proteins from the ES cells were analyzed. The G418-sensitive feeder cells were typically eliminated after 2 days of exposure to G418.
18. C. A. Mizzen and C. D. Allis, *Cell. Mol. Life Sci.* **54**, 6 (1998); K. Struhl, *Genes Dev.* **12**, 599 (1998).
19. T. Nakajima et al., *Cell* **86**, 465 (1996).
20. V. V. Ogryzko, R. L. Schiltz, V. Russanova, B. H. Howard, Y. Nakatani, ibid. **87**, 953 (1996); A. J. Bannister and T. Kouzarides, *Nature* **384**, 641 (1996).
21. A. S. Alberts, O. Geneste, R. Treisman, *Cell* **92**, 475 (1998).
22. Fibroblasts were maintained in serum-free medium for 1 to 2 days before stimulation. After treatment, cells were washed twice in cold phosphate-buffered saline (PBS) and lysed directly in boiling SDS sample buffer. Cell lysates were resolved by SDS-PAGE (8 or 10% gels); equal loading was confirmed by staining parallel gels with Coomassie blue. Resolved samples were electroblotted onto PVDF membranes, and equal transfer was confirmed by staining blots with Ponceau S. Membranes were blocked in 5% low-fat dry milk in PBS for 2 hours at room temperature and then incubated with primary antibody for 12 hours at 4°C. Membranes were washed five times in PBS before incubation with peroxidase-conjugated secondary antiserum for 2 hours at room temperature. After five washes in PBS, immunocomplexes were detected by enhanced chemiluminescence.
23. Equivalent numbers of normal and CLS fibroblasts were seeded on separate cover slips within 60-mm culture dishes and grown for 24 hours. Cells were then serum-starved for 24 hours, mock-treated or treated with EGF (50 ng/ml) for 30 min, and fixed in PBS (pH7.5) containing 4% paraformaldehyde. Fixed cells were permeabilized with PBS containing 0.2% Triton X-100, blocked with 2% goat serum in PBS, and sequentially incubated with the pS10 antiserum and rhodamine- or fluorescein-conjugated goat anti-rabbit secondary antisera. Immunostained cells were counterstained with 4,6-diamidino-2-phenylindole (DAPI) before microscopy. Cells stained with rhodamine-conjugated secondary antiserum were photo-graphed and color prints were scanned in RGB mode to generate electronic image files. Cells stained with fluorescein-conjugated secondary antiserum were captured as grayscale images by using a charge-coupled device camera. Both types of files were converted to CMYK images and colorized with Adobe Photoshop.
24. NIH 3T3 cells were cultured in Dulbecco's modified Eagle's medium (DMEM) containing fetal bovine serum (FBS, 10%). When cells were ~80% confluent, growth medium was replaced with DMEM without serum. Typically, cells were serum-starved for 24 hours before mitogen stimulation. Normal human and CLS (Rsk-2 deficient) fibroblasts, immortalized with Epstein-Barr virus (*14*), were cultured as above. The CLS cells used in this study are derived from a patient in which a splice site mutation leads to the use of a cryptic acceptor site and premature termination at amino acid 422. Consequently, Rsk-2 protein in these cells lacks the second kinase domain and is inactive (*14*, *15*). Stimulation with EGF (50 ng/ml, Sigma) was performed as described (*5*, *15*).
25. Cells were harvested and washed twice in nucleus isolation buffer (NIB) containing 15 mM tris-HCl (pH 7.5), 250 mM sucrose, 60 mM KCl, 15 mM NaCl, 5 mM MgCl₂, 1 mM CaCl₂, 0.1% (v/v) β-mercaptoethanol, 2 mM sodium vanadate, and a protease mixture containing 2.5 μg/ml each of leupeptin, pepstatin, aprotinin, antipain, and chymostatin (Sigma) as well as 1 mM phenylmethylsulfonyl fluoride (Sigma). Cells were lysed in NIB containing 0.6% NP-40 (v/v), and the nuclei were collected by centrifugation at 3000 rpm for 5 min at 4°C and gently resuspended in NIB. The nuclei were washed three times (or more) in NIB to minimize contaminating extranuclear debris. Nuclear extracts were prepared as described [J. D. Dignam, R. M. Lebovitz, R. G. Roeder, *Nucleic Acids Res.* **11**, 1475 (1983)]. Acid-soluble proteins were prepared by extracting H3 with 0.4 N H₂SO₄.
26. Kinase activity gel analyses were done as described [J. E. Brownell and C. D. Allis, *Proc. Natl. Acad. Sci. U.S.A.* **92**, 6364 (1995)] except that the separating portions of the gels contained 8% acrylamide and reversed-phase high-performance liquid chromatography (rpHPLC)–purified chicken erythrocyte histone H3 or calf thymus H3 (0.1 mg/ml, Boehringer). Similar results were obtained with gels containing the nonphosphorylated H3 NH₂-terminal peptide (Fig. 1B). Gels were renatured overnight at 4°C in buffer containing 30 mM MOPS-NaOH (pH 7.4), 100 mM NaCl, 5 mM MgCl₂, 2 mM MnCl₂, 1 mM dithiothreitol (DTT), 0.05% (v/v) NP-40, allowed to come to room temperature, and then washed in assay buffer [30 mM MOPS-NaOH (pH 7.4), 5 mM MgCl₂, 2 mM MnCl₂, 1 mM DTT] for two 30-min intervals. Gels were then sealed in polyethylene bags containing 3 ml of assay buffer and 100 μCi of [γ-³²P]ATP (adenosine 5'-triphosphate) (3000 Ci/mmol, NEN), and incubated on a rocking platform at 30°C for 4 hours. After extensive washing in 1% (w/v) tetrasodium pyrophosphate, gels were stained with Coomassie blue R-250 and destained before autoradiography.
27. Histone substrates were prepared by acid extraction of isolated chicken erythrocyte nuclei. Individual histone fractions were purified by rpHPLC. Chromatin fractions were prepared by sucrose density centrifugation of chromatin solubilized by micrococcal nuclease digestion of isolated chicken erythrocyte nuclei. Conventional kinase assays used the protocol supplied with an S6 kinase assay kit (Upstate Biotechnology). Where appropriate, portions of assay mixtures were recovered by trichloroacetic acid (TCA) precipitation (20% final) or supplemented with 5× sample buffer, resolved by SDS-PAGE (12% gels), and processed for autoradiography or protein immunoblotting.
28. rpHPLC-purified chicken erythrocyte H3 (1 μM) was incubated with 1 U of rabbit Rsk-2 in 250 μl (final) of assay buffer containing 50 μCi of [γ-³²P]ATP for 90 min at 30°C. The sample was recovered by TCA precipitation and H3 purified by rpHPLC before microsequence analysis. Sequencing was performed as described [Y. Wei, C. A. Mizzen, R. G. Cook, M. A. Gorovsky, C. D. Allis, *Proc. Natl. Acad. Sci. U.S.A.* **95**,

7480 (1998)]. The repetitive yield for the analysis shown in Fig. 2B was 92%.

29. Cells in DMEM containing FBS (10%) were initially arrested at the G_1/S boundary by exposure to aphidicolin (5 μg/ml) for 12 hours. Cultures were then washed with PBS and allowed to grow for 3 hours in DMEM containing 10% FBS. Cells were then arrested at the G_2/M boundary by exposure to nocodazole (0.05 μg/ml) for 12 hours. The cultures were then washed and incubated with fresh DMEM without serum for 6 or 24 hours before stimulation with EGF (100 ng/ml) for 30 min. Lysates were prepared and analyzed by immunoblotting (22).

30. Parallel cultures of CLS cells (in 60-mm culture dishes) at 80% confluency were transfected either with 1.0 μg of vector DNA (pSG5) [S. Green, I. Issemann, E. Sheer, Nucleic Acids Res. **16**, 369 (1988)] or with 1.0 μg of the human Rsk-2 expression plasmid pTHL-Rsk2 (human Rsk-2 cDNA cloned into the pSG5 vector) by using Lipofectamine Plus transfection reagent (Life Sciences). Transfected cells were cultured in medium containing 10% FBS for 24 hours and then in serum-free medium for another 24 hours. Cells were then mock-treated or treated with EGF (50 ng/ml) for 30 min before harvesting. Lysates were prepared and analyzed by immunoblotting (22). For immunofluorescence analyses, CLS cells were grown on cover slips in 60-mm dishes and transfected as described above. Indirect immunofluorescence was performed as described (23).

31. Protein microsequencing and peptide synthesis were done at Baylor College of Medicine (Houston, TX) by R. G. Cook. We thank J. Davie, D. De Cesare, M. J. Hendzel, L. Mahadevan, K. Merienne, M. Montminy, and A. Vertegal for helpful discussions; E. Heitz and J. Zhou for technical assistance; and T. Parsons and T. Sturgill for comments on this manuscript. Supported by grants to C.D.A. (NIH-GM40922) and P.S.-C. (Centre National de la Recherche Scientifique, Institut National de la Santé et de la Recherche Médicale, Centre Hospitalier Universitaire Régional, Fondation de la Recherche Médicale, and Association pour Recherche sur le Cancer).

The Selective Advantage of Low Relatedness

Blaine J. Cole and Diane C. Wiernasz

Relatedness within colonies of social Hymenoptera is often significantly lower than the outbred population maximum of 0.75. Several hypotheses address the widespread occurrence of low relatedness, but none have measured the co-variation of colony fitness and relatedness. In a polyandrous harvester ant, *Pogonomyrmex occidentalis*, average within-colony relatedness in the population is low but highly variable among colonies, and relatedness is negatively correlated with colony growth rate. Differences in growth rate strongly influence survival and the onset of reproduction, leading to a 35-fold increase in fitness of fast-growing colonies. Benefits of a genetically diverse worker population may favor polyandry in this species.

The relation between genetic relatedness and altruism has dominated modern studies of social behavior, especially in the social Hymenoptera where asymmetries in relatedness among male and female offspring and among queens and workers shape interactions (1). Technical advances in the estimation of relatedness have allowed social insect biologists to study the relation between relatedness and many aspects of reproductive allocation and behavior (2–4).

Although high within-colony relatedness promotes the spread of altruistic traits and may favor many types of social behavior, the diversity of social systems among social insects (from singly mated, single queens to multiply mated, multiple queens) produces a corresponding diversity of relatedness values. To explain such diversity, a number of hypotheses have been proposed that identify potential advantages to low relatedness (5). Low relatedness that arises from polyandry (multiple mating by queens) is of particular interest, because polyandry is taxonomically widespread. Data from natural populations comparing relatedness to aspects of fitness are virtually absent (6, 7).

We have studied the western harvester ant *Pogonomyrmex occidentalis*. Colonies of this species are founded by a single queen (8); variation in the mating frequency of queens produces variation in colony relatedness. We genotyped six workers from each of 1492 colonies (9) over a 4-year period at two variable loci, phosphoglucose isomerase (PGI) and amylase (AMY) (10). Within-colony relatedness was estimated individually from the combined electrophoretic data (11). The average relatedness in the population is 0.324 ± 0.017 (mean ± SE, $n = 1128$ colonies collected in 1993). We censused colonies annually between 1993 and 1998 and measured colony size (12) in 1993, 1994, 1997, and 1998 to determine survival and growth. Colony growth rate was correlated in all years with colony size: Small colonies grew more rapidly than large colonies (1993–1994: $r = -0.33$; 1994–1997: $r = -0.59$; 1997–1998: $r = -0.34$). We used the residuals of the regression of growth on size in a given time interval to estimate colony growth corrected for current size for that interval (13).

Relatedness and residual colony growth are negatively correlated for every time interval (1993–1994: Spearman rank correlation $r_s = -0.0908$, $n = 927$, $P = 0.0057$; 1994–1997: $r_s = -0.0789$, $n = 809$, $P = 0.025$; 1997–1998: $r_s = -0.0243$, $n = 791$, $P = 0.495$). Overall, the relation is strongly negative [combining these probabilities by using Fisher's method (14), $\chi^2 = 19.12$, df = 6, $P < 0.005$]. Total growth over the 5-year period 1993 to 1998 is also negatively correlated with colony relatedness ($r_s = -0.102$, $n = 646$, $P = 0.0095$) (Fig. 1). Although significant, the correlation between growth and relatedness is not very large. Our estimate of average colony relatedness for the entire population is accurate, but the estimates for individual colonies have large standard errors (2, 3). On the assumption that the correlation between colony relatedness and growth is due to a correlation between the actual growth and actual
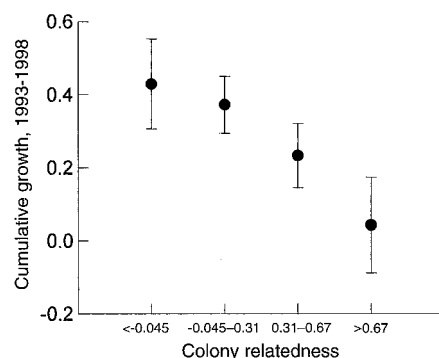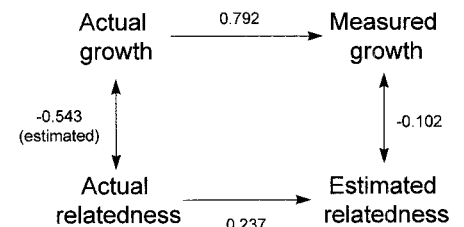

Fig. 1. The relation between colony growth and colony relatedness. Colony growth is the residual growth over the 5-year period 1993 to 1998. Colonies are categorized by their within-colony relatedness as being more than 1 SD (SD = 0.356) below the mean individual relatedness (0.315), within 1 SD below the mean, within 1 SD above the mean, and more than 1 SD above the mean.

Fig. 2. The path analysis estimate of the relation between colony growth and colony relatedness. The correlation between actual growth and measured growth is based on the correlation between colony size and our measure of colony size (8), and the correlation between estimated and actual relatedness for individual colonies is estimated from simulations (14). The correlation between measured growth and estimated relatedness is the correlation with growth over a 5-year period.

Division of Evolutionary Biology and Ecology, Department of Biology and Biochemistry, University of Houston, Houston, TX 77204–5513, USA. E-mail: bcole@uh.edu